J Mater Sci (2010) 45:4390–4400
DOI 10.1007/s10853-010-4429-0

EUROMAT 2009

The influence of salt fog exposure on the fatigue performance of Alclad 6xxx aluminum alloys laser beam welded joints

A. T. Kermanidis · A. D. Zervaki · G. N. Haidemenopoulos · Sp. G. Pantelakis

Received: 14 November 2009 / Accepted: 18 March 2010 / Published online: 3 April 2010

Abstract Laser welding is increasingly used for the fabrication of lightweight and cost-effective integral stiffened panels in modern civil aircraft. As these structures age in service, the issue of the effect of corrosion on their damage tolerance requires attention. In this work, laboratory data on the influence of salt fog corrosion on the fatigue behavior of cladded 6156 T4 aluminum alloy laser welded specimens are presented. The experimental investigation was performed on 6156 T4 laser butt welded sheets. Prior to fatigue testing the welded joints were exposed to laboratory salt fog corrosion exposure for 720 h. The results showed that the clad layer offers sufficient corrosion protection both on base metal and the weld. Fatigue testing was followed by standard metallographic analysis in order to identify fatigue crack initiation sites. Crack initiation is located in all welded samples near the weld reinforcement which induces a significant stress concentration. Localized corrosion attack of the clad layer, in the form of pitting corrosion, creates an additional stress concentration which accelerates crack initiation leading to shorter fatigue life relative to the uncorroded samples. The potency of small corrosion pits to act as stress concentration sites has been assessed analytically. The above results indicate that despite the general corrosion protection offered by the clad layer, the localized attack described above leads to inferior fatigue performance, a fact that should be taken under consideration in the design and maintenance of these structures.

A. T. Kermanidis · A. D. Zervaki (✉) ·
G. N. Haidemenopoulos
Department of Mechanical Engineering, University of Thessaly,
38334 Volos, Greece
e-mail: azerv@uth.gr

Sp. G. Pantelakis
Laboratory of Technology and Strength of Materials (LTSM),
Department of Mechanical Engineering and Aeronautics,
University of Patras, 26500 Rion, Patras, Greece

Introduction

Laser welding is a new, promising technology in aluminum airframes towards weight saving and cost efficient design. Although laser welded parts are increasingly used in modern aircraft, the technology is not considered yet for highly loaded parts, which require superior damage tolerance characteristics. One of the important issues for consideration of laser welding in demanding damage tolerant applications is the thorough understanding of the welded joints corrosion behavior, as it is a serious threat to its fatigue resistance, especially in aging aircraft. This is particularly important when one considers interactions of corrosion with: (i) weld defects, (ii) stress concentrations imposed by geometrical discontinuities in the welded joint, (iii) tensile residual stress fields in the vicinity of the weld. The laboratory and field data on the issues stated above are scarce, particularly for laser welded airframe alloys used in civil aircraft. This work aims to contribute with valuable laboratory data to a better understanding on the influence of corrosion on the fatigue performance of the laser welded 6156 T4 airframe alloy.

Corrosion behavior of welded joints can be influenced by the dissimilar microstructures at the weld region including the weld metal, heat affected zone, partially melted zone, and base metal. The authors of the present paper presented evidence [1] that dissimilar microstructures can be the cause of localized corrosion in the case of 2139 aluminum laser beam welds. Corrosion properties of laser hybrid welds in AA 6061 have been reported in [2].

Corrosion attack is hindered by the use of cladding or anodizing, which can offer sufficient corrosion protection even in aggressive laboratory corrosive environments [3, 4]. It is also well known that cladding of Alclad products electrochemically protects the core at exposed edges and at abraded or corroded areas [5]. Scratch tests performed in [6] confirmed that surrounding cladding sufficiently protects the core material at the areas of scratches made on cladded aluminum specimens, prior to their exposure to salt spray fog. Furthermore, the works in [3, 6] provided evidence that only locally cladded specimens have been sufficiently protected against corrosion also at their areas which did not provide a clad layer. This observation is important for understanding the corrosion susceptibility of the laser welded joints. Still, in long term operation the protective cladding can deteriorate due to cyclic mechanical loads, environmental attack, or combination of the former [7, 8]. Experimental investigations exist, which show evidence of the corrosion susceptibility of the clad layer following exposure to laboratory corrosion [4], and clad layer failure due to cracking under applied fatigue loads [7, 9, 10]. A protective layer, damaged either by corrosion or fatigue, can assist the further development of corrosion, or promote the degradation of the substrate fatigue properties, thus leading to the condition of an aged structure. Damage tolerance behavior of aged aircraft materials has been a subject of investigation by many researchers and attention has been focused on the fatigue behavior of pre-corroded aluminum alloys [11–15]. On the other hand, experimental results on the fatigue behavior of aged, welded aluminum-joints are very limited. The authors of this study presented experimental results in [1] indicating that prior corrosion exposure leads to fatigue resistance degradation in bare 2139 aluminum alloy laser welded samples. The reason has been localized stress concentration at corrosion pits, which acts in synergy with the stress concentration induced by the notch at the weld toe and results in premature crack initiation and reduction of fatigue life. The corrosion behavior observed was strongly related to the temper condition affecting the corrosion susceptibility of the 2139 alloy.

In the current investigation, the influence of existing corrosion damage on the fatigue performance of cladded 6156 T4 aluminum laser welded specimens was examined. First, the corrosion susceptibility of the welded specimens was evaluated after exposure to salt fog environment and the protective role of the clad layer was assessed. Next, the influence of corrosion exposure on fatigue behavior of 6156 aluminum welded joints was investigated. For this purpose, evaluation of the fatigue results was performed in terms of stress versus number of cycles (S–N) fatigue curves. The effect of localized corrosion damage at the clad layer on the fatigue life of corroded welded joints was investigated and supported with metallographic and fractographic examination. Fatigue crack initiation sites and fracture path were identified with assistance of fractography. The role of stress concentrations arising from the weld reinforcement and localized corrosion of the clad layer was evaluated. Finally, the elastic stress concentration factors and associated local stresses at the weld toe and around corrosion pits responsible for crack initiation have been calculated analytically and used to explain the obtained fatigue results.

Experimental

The butt-welded sheets were received from Gesellschaft zur Förderung der Kernenergie in Schiffbau und Schiffstechnik (GKSS) research centre (Germany) with dimensions of 270 × 315 mm. The thickness of the sheets was 2.8 mm. The chemical composition of the base metal was (wt%) Si 1, Mg 0.9, Cu 0.9, Fe 0.1, Mn 0.55, Cr 0.125, and Zn 0.4. Prior to welding the sheets were tempered to T4 condition which includes solution heat treatment and natural aging to substantially stable condition. A diode-pumped 3.3 kW Nd:YAG laser DY033 from Rofin-Sinar was employed for the welding experiments. Laser power was adjusted at 3000 W, and the focal point position was on the top of the sheet. Spot size in focus was 0.4 mm. The welding speed was 1.8 m/min. Filler wire 4047 (12.25% Si, 0.6% Fe, 0.05% Cu, 0.25% Mn, 0.05% Mg, 0.1 %Zn, 0.1% Ti) of 1.2 mm diameter was used at a feed rate of 2.5 m/min. Surface protection was achieved by supplying 25 l/min He, while Ar was used for root protection at 15 l/min.

Machining of the fatigue specimens was performed according to the ASTM E 466 specification [16]. All specimens were cut in the longitudinal (L) orientation relative to the rolling direction. Fatigue tests were performed with a stress ratio $R = 0.1$ and a frequency of 25 Hz on corroded and uncorroded welded specimens for comparison.

Prior to fatigue testing the specimens were exposed to salt fog environment in a salt spray chamber according to the ASTM B117 standard [17]. A continuous corrosion exposure in the salt fog for 720 h was applied in order to cause sufficient corrosion damage for the fatigue performance investigation. The sodium chloride (NaCl) concentration used for the accelerated corrosion exposure was 5% mass. Throughout the test it was ensured that inside the chamber the temperature range was maintained at 35 ± 1 °C, while the pH was maintained between 6.5 and 7.2. After exposure, the specimens were cleaned according to ASTM G1 specification [18].

Standard metallographic techniques (including grinding and polishing) were applied for the characterization of

microstructures in the base material, heat affected zone, and weld metal. Etching was performed by using Keller's reagent. Microhardness measurements in all weld sections were performed using a Vickers indenter and a load of 0.2 kg.

Results

Materials

The microstructure of the clad 6156 alloy is shown in the macrograph of Fig. 1. The structure consists of Al-rich grains elongated towards the rolling direction, associated with rounded Mg_2Si particles. Clad layer has an average thickness of 60 μm.

A typical microhardness profile is shown in Fig. 2, where the distinct weld zones are indicated, i.e., weld metal (WM), partially melted zone (PMZ), heat affected zone (HAZ), and the unaffected material (BM). A continuous hardness drop is observed as approaching the WM from the BM. This is associated with the dissolution and coarsening of the strengthening precipitates in the HAZ [19], while within the PMZ the hardness drop is associated with dissolution of the strengthening phases and the formation of eutectic constituents [1].

Corrosion behavior

After exposure in the salt fog environment, metallographic examination of the corroded welded samples was performed. Images obtained with the use of optical microscopy revealed that even after the relatively long exposure time of 720 h in NaCl fog, the weld metal was free of corrosion attack (Fig. 3a). The clad layer acted as a sacrificial anode offering sufficient corrosion protection to the weld metal. This is supported by evidence of small-scale, pitting corrosion damage, found on the clad layer as shown in Fig. 3b. The average and maximum pit depth has been

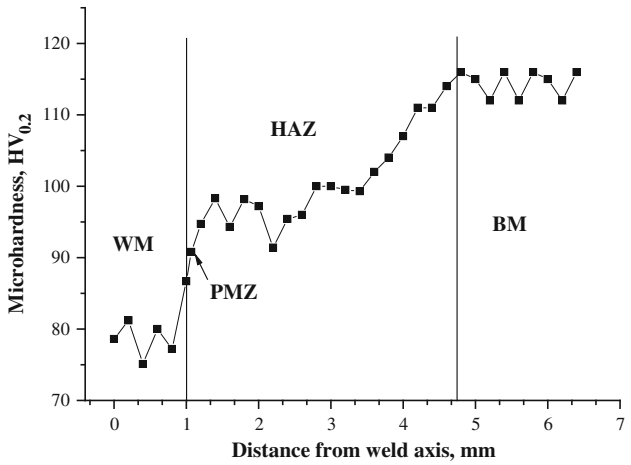

Fig. 2 Microhardness profile across the weld bead in 6156-T4 alloy

estimated at 5.22 and 11.95 μm, respectively. The pit depth values are average values of several measurements performed on the metallographic specimens. Pitting corrosion has been also found at the base metal, near the interface with the weld reinforcement (Fig. 3c). The role of the clad layer observed in terms of corrosion behavior is similar to the operation of the local cladding pattern, first described in [3] as a potential alternative, cost efficient method to provide corrosion protection in aluminum alloys.

Fatigue results

Taking into consideration that machining of specimens from the rolled welded sheet causes a relief of the weld residual stresses [20], the fatigue results in the following section are discussed with neglecting any effects caused by residual stresses. In addition, the welded samples were tested in fatigue as received, without mechanical removal of the weld reinforcement in order to investigate on the role of stress concentrations induced by geometrical factors such as the weld toe and root reinforcement on the fatigue behavior of welded samples.

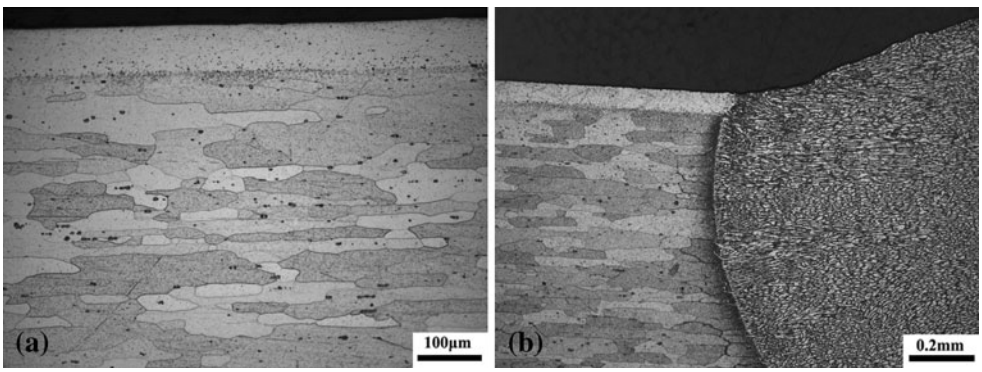

Fig. 1 Typical microstructures of clad 6156 T4 **a** base metal **b** weld region

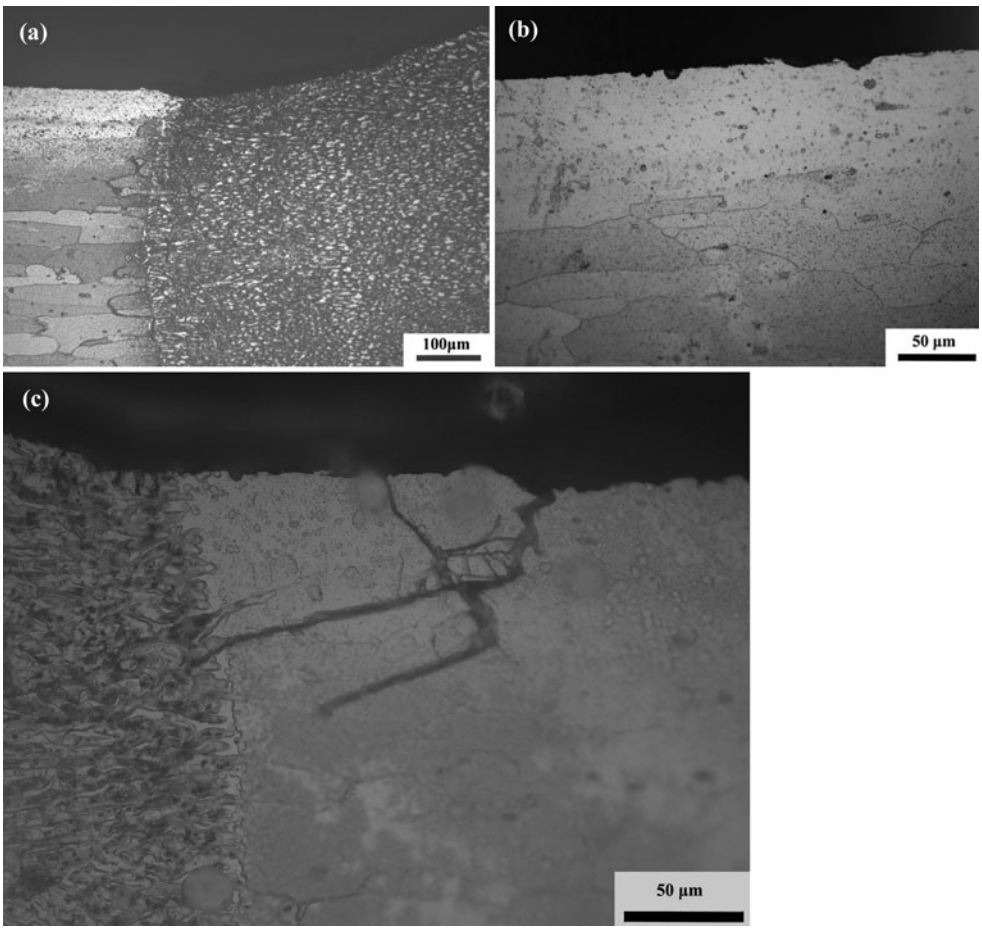

Fig. 3 Micrographs of weld and base metal area after 720 h exposure to salt fog **a** corrosion free weld metal **b** corrosion pits at the clad layer, at the base metal area, **c** corrosion pits at the interface base metal–weld reinforcement

Constant amplitude cyclic tests were performed with a stress ratio of $R = 0.1$ and a frequency of 25 Hz with the use of a servohydraulic 100 kN fatigue testing machine. Two fatigue specimens have been tested at each stress level. The fatigue results are displayed in the form of *S–N* experimental data fitted to a 4-parameter Weibull distribution. The experimental results show a harmful effect of corrosion on the fatigue behavior of welded specimens. The fatigue behavior given in Fig. 4 in terms of *S–N* curves is degraded for the corroded joints, which exhibit shorter fatigue lives compared to the uncorroded welded specimens for all stress levels examined. The *S–N* Weibull fitting curves lead to a fixed fatigue limit at 10^7 cycles of 100 and 80 MPa for the uncorroded and corroded welded joints, respectively. It corresponds to a fatigue limit reduction of 20% for the aged welded joints. The average % reduction in fatigue life for the corroded specimens is 65% obtained at fatigue stress levels of 100–150 MPa.

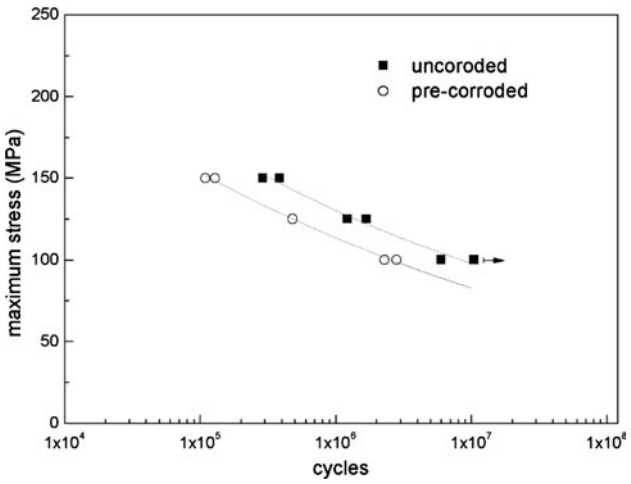

Fig. 4 Fatigue results (*S–N* curves) of uncorroded and pre-corroded 6156 T4 welded joints

In both uncorroded and corroded welded joints, fatigue fracture occurred at the boundary of weld reinforcement with base metal as shown in Fig. 5. The weld toe stress concentration plays a principle role, leading to controlled fatigue crack initiation in this area. The considerable shortened fatigue lives of the corroded specimens

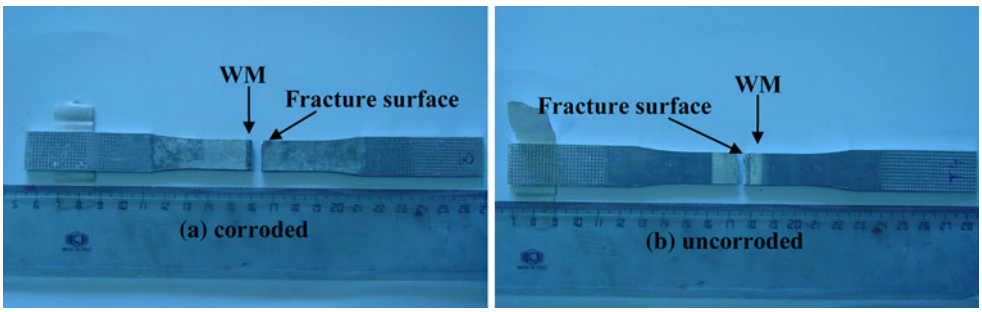

Fig. 5 Fractured specimens indicating fatigue fracture at the weld boundary regions for **a** corroded and **b** uncorroded welded joints

presented in Fig. 4 indicate that despite the induced stress concentration at the weld toe, corrosion introduces an additional effect which further degrades fatigue crack initiation resistance. Herein, the role of pitting corrosion seems to be critical for the fatigue behavior of corroded welded joints. Evidence on this observation is provided in a following section of this paper.

To support the obtained experimental results and rationalize the effect of corrosion on the fatigue behavior, further evaluation of the main factors influencing the cyclic behavior has been performed. The evaluation performed and described in the next paragraphs consists of two parts. First, fractographic investigation combined with metallography on sections of the welded joint was performed in order to identify the exact fatigue crack initiation sites and propagation of fatigue damage. Next, the effects of stress concentrations at the weld reinforcement and at corrosion pits have been estimated and their role on fatigue crack initiation has been assessed.

Fractographic investigation

From stereoscopic examination, the fatigue section, as well as, the fast fracture area on specimen fractured surfaces were identified. In most cases fatigue section has the typical semi-elliptical shape with the center being the fatigue initiation site (Figs. 6b, 10b). In order to determine the crack initiation site, cross sectioning was performed exactly at the center of the fatigue section area. Fractographic observations in both uncorroded and pre-corroded samples revealed that cracks initiate at the weld toe or weld root of the specimen, at the interface of the partially melted zone (PMZ) with the weld metal, and propagate perpendicular to the stress axis (mode I) until final fracture (Fig. 6a, c). Inspection of the fracture surfaces revealed the typical appearance of a fatigue section initiated at the weld toe or weld root, followed by a final fast fracture area, as shown in Fig. 6b.

Secondary microcracks initiating at the weld boundary were also observed. As shown in Fig. 7, they propagate in a depth exceeding the clad layer thickness and then are arrested. Final failure is dominated by the principle crack, which initiates at a different location of the weld boundary and propagates until fracture. While in the uncorroded samples, secondary cracks formed only at the boundary of weld reinforcement, in the case of corroded samples secondary cracks were also observed far from the stress concentration region (Fig. 8). The clad layer material is AA1300, with 80 MPa yield strength and 70 GPa modulus of elasticity. The modulus of the clad layer is similar to that of the base material 6156. Hence the fatigue stresses applied at the clad layer and base metal are equal, reaching and exceeding, in some cases, the tensile strength of the clad layer. Also, it should be expected that after 720 h exposure to salt fog the small corrosion pits observed at the clad layer surface give the aluminum layer a more brittle behavior under tensile loads. The above conditions may explain the preferential cracking observed in the corroded samples in opposition to the uncorroded samples at remote surface regions with regard to the weld toe boundary. However, the observed cracking at these locations does not prove to be essential for fatigue behavior, since it's effect is overwhelmed by the effect of stress concentration at the weld toe.

Corrosion pits at the clad layer have an additional influence on fatigue crack initiation occurring at the weld reinforcement boundary. Fatigue cracks in the corroded specimens initiate at the bottom of corrosion pits at the PMZ as depicted in Fig. 9. Then, as in the case of uncorroded samples, they propagate perpendicular to the applied load until final fracture. Again, inspection of the fracture surfaces revealed the typical appearance of a fatigue section initiated at the weld toe, followed by a final fast fracture area, as shown in Fig. 10.

In the previous analysis, the experimental results reveal the harmful influence of corrosion on the fatigue performance of welded joints. Taking under consideration, that: (i) fatigue crack initiation occurs always in the PMZ at the

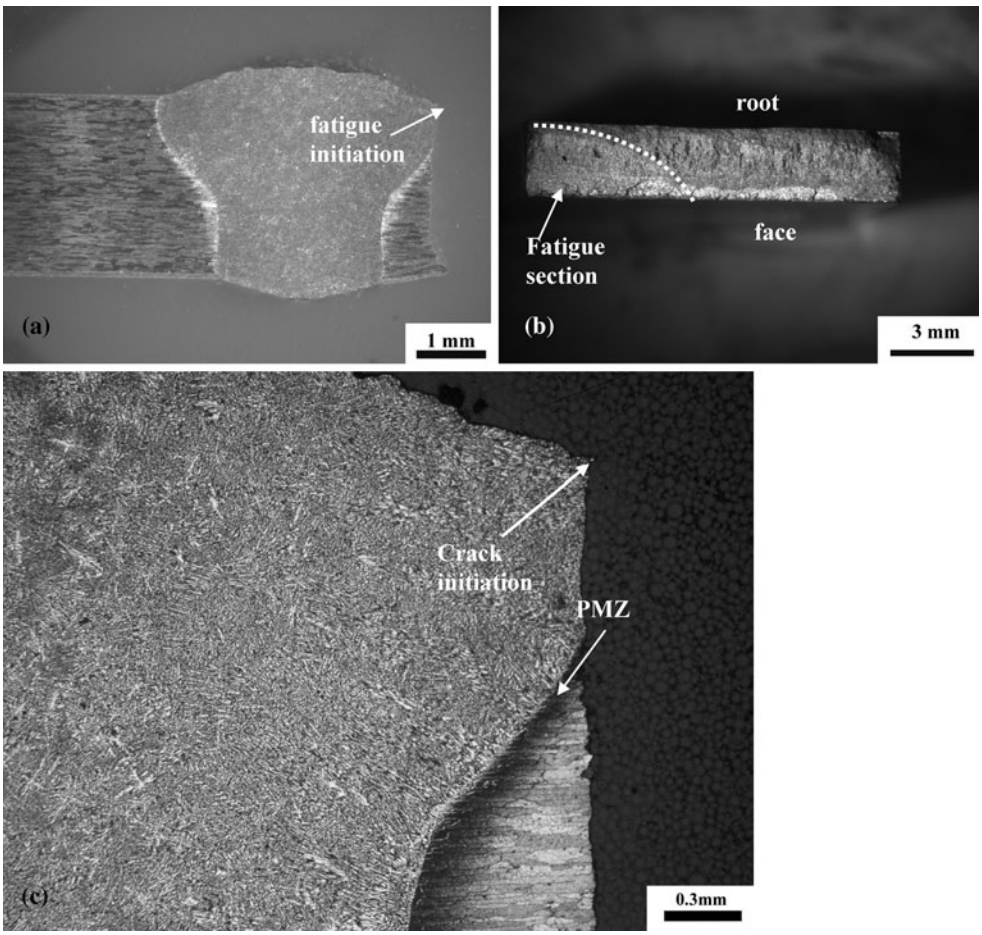

Fig. 6 **a** Location of fatigue crack initiation and propagation, **b** fatigue section followed by brittle fracture, **c** crack propagation at the PMZ–weld metal interface

weld metal–base metal interface, (ii) fatigue crack initiation is generated around corrosion pits in the corroded samples, the observed fatigue behavior may be explained under the viewpoint of a combined, pronounced stress concentration effect caused by the co-existence of weld toe and corrosion pits at the same location. In order to support the experimental findings, the local stress at the weld reinforcement boundary has been estimated and compared to the localized stress around the corrosion pit. For this purpose, the elastic stress concentration factors have been calculated for the distinguished effects and are presented in the following section.

Estimation of local stress at crack initiation location

Estimation of local stress at weld toe

The stress concentration created by the existence of weld reinforcement is dominant in the fatigue behavior and facilitates crack initiation at the boundary of weld toe and base metal. To calculate the local stress induced by the presence of the weld toe/root, the elastic stress concentration factor due to the notch effect introduced by the weld toe has been calculated analytically. For the estimation of the elastic stress concentration factor at the weld toe, the analytical solutions by Lehrke et al. [21, 22] and Ushirokawa and Nakayama [23] have been implemented. For a butt weld in tension, Lehrke presented the following equation for the elastic stress concentration factor at the weld toe:

$$K_{t1} = \frac{4\left(2\tan\frac{\theta}{2}\right)^{1-2m}}{2\theta + \sin(2\theta)}\left(\frac{t}{4\rho}\right)^{m} \quad (1)$$

with $W = t$. This condition is in agreement with the weld joint configuration in the present study as shown in Table 1.

The parameters W, θ, ρ, and t displayed in Fig. 11 are given in Table 1 for the welded joint configuration under investigation. For a butt weld under combined tension and bending, Ushirokawa and Nakayama [23] proposed the

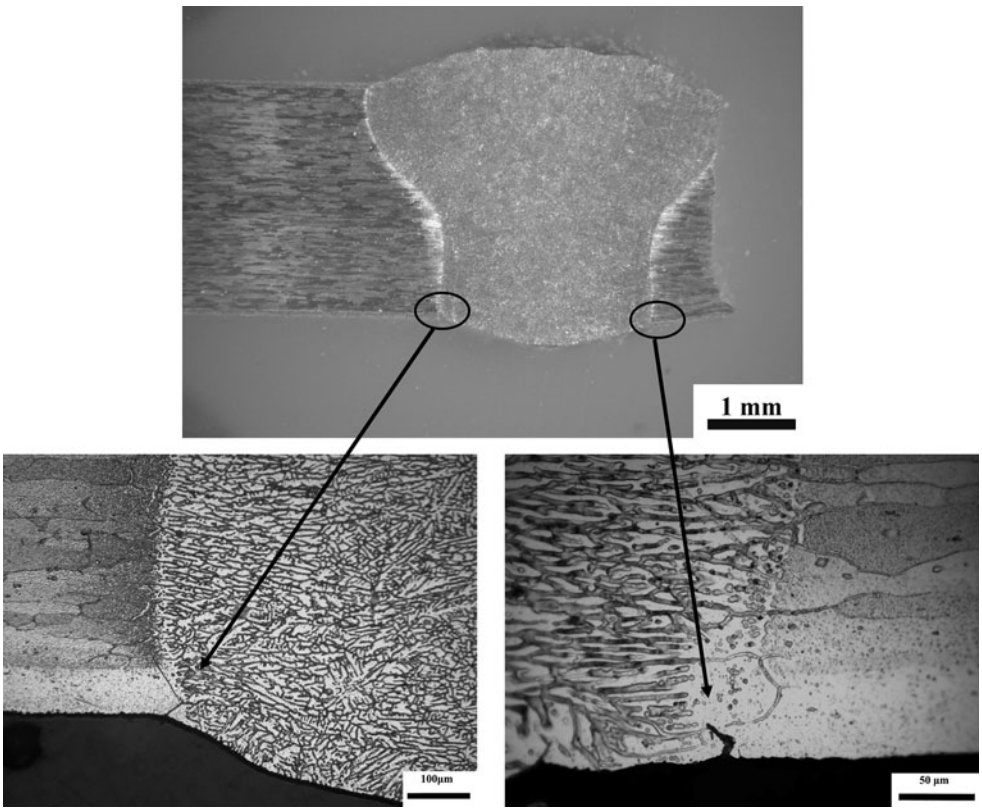

Fig. 7 Secondary cracks initiate at the weld root boundary

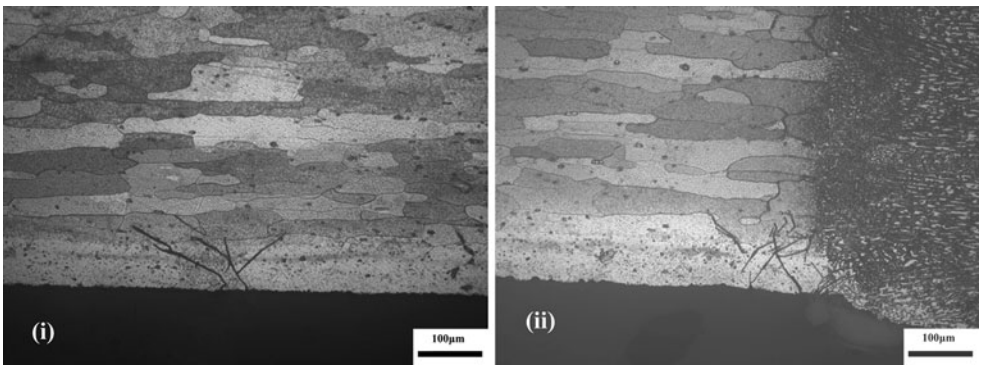

Fig. 8 Secondary cracking observed (i) far from weld root boundary, (ii) at weld root boundary

following equation for the calculation of the elastic stress concentration factor at the weld toe:

$$K_{t2} = [1 + f(\theta)\{g(\rho) - 1\}]C(a/t) \tag{2}$$

with

$$f(\theta) = \frac{1 - \exp\left\{-0.90(\pi - \theta)\sqrt{\frac{W}{2h}}\right\}}{1 - \exp\left\{-0.90(\pi/2)\sqrt{\frac{W}{2h}}\right\}}, \tag{3}$$

In Eq. 2 $g(\rho) = \alpha_t g_t(\rho) + a_b g_b(\rho)$, and $C(a/t)$ is the parameter for lack of penetration. In the present analysis no lack of penetration has been considered hence the value $C(a/t) = 1$ was taken.

By neglecting bending and lack of penetration then $g_b(\rho) = 0$ and $\alpha_t = 1$ In this manner:

$$g(\rho) = g_t(\rho) = 1 + \beta_t \left\{(h/\rho)\,\frac{1}{2.8(W/t) - 2}\right\}^{0.65} \tag{4}$$

with

$$W = t + 2h + 0.6h_p \tag{5}$$

The value of β_t for the butt joint configuration is $\beta_t = 2$ [23].

The parameters W, h, θ, ρ, and t displayed in Fig. 12 are given in Table 1 for the welded joint configuration under investigation.

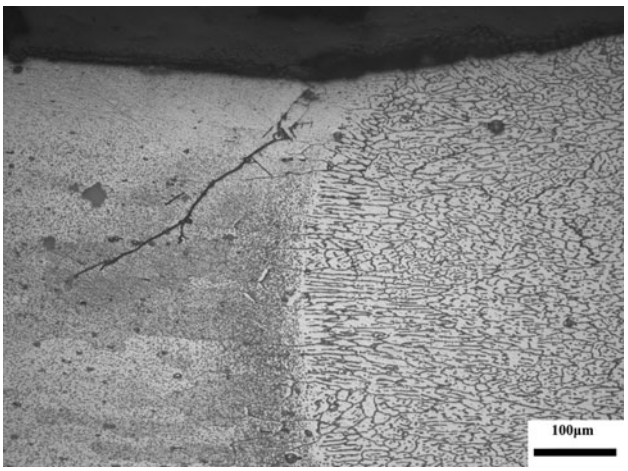

Fig. 9 Crack initiation at the bottom of corrosion pit at the PMZ

With the use of Eqs. 1 and 2 and the parameters given in Table 1 the values of stress concentration factors have been calculated $K_{t1} = 1.62$ and $K_{t2} = 1.54$, respectively. Both equations result in similar elastic stress concentration values at the weld toe of the butt joint.

Estimation of local stress around corrosion pit

In the corroded welded joints premature initiation of fatigue cracks leading to reduction of fatigue life was attributed to the presence of corrosion pits at the clad layer resulting to a supplementary local stress concentration at the bottom the pit adjacent to the weld reinforcement.

To estimate the value of the elastic stress concentration factor at the bottom of a corrosion pit, the pit has been simulated as a small surface semi-circular notch with radius of curvature r. In the case of a surface, semi-circular notch in tension the elastic stress concentration factor can be derived with the use of the equation suggested by Cole et al. [24]

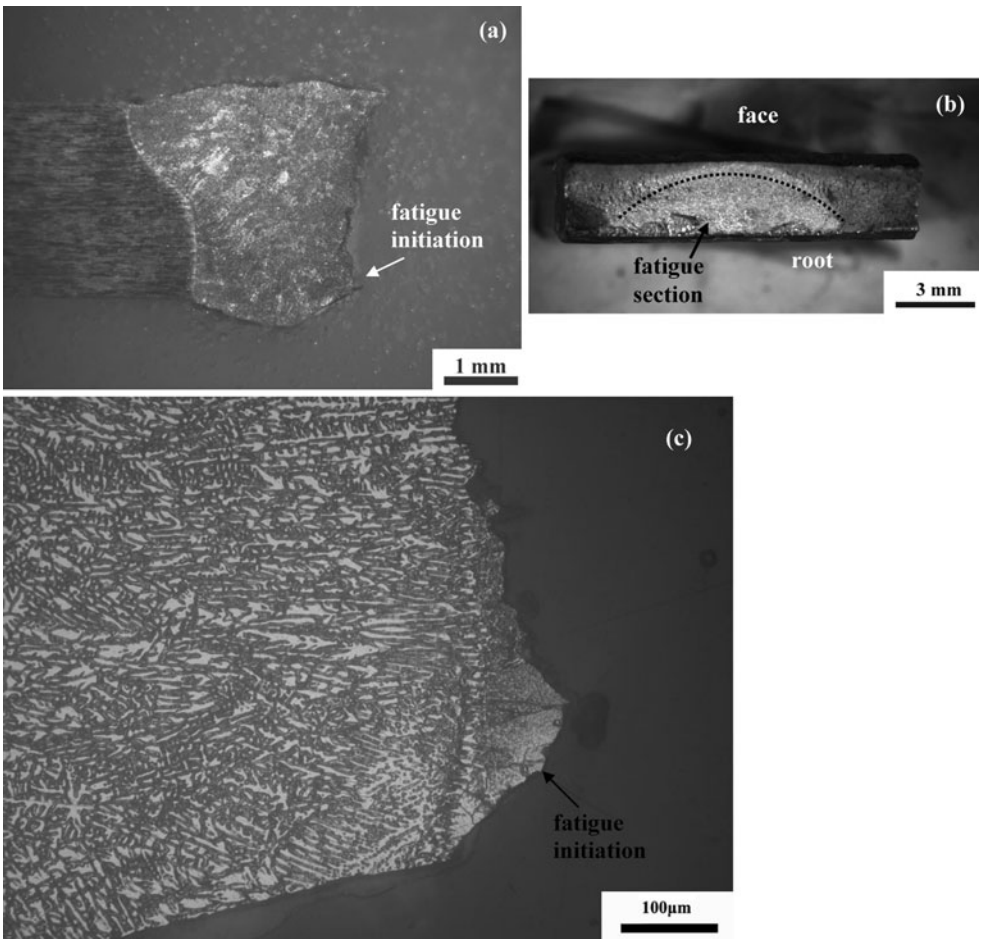

Fig. 10 **a** Location of fatigue crack initiation and propagation, **b** fatigue section followed by brittle fracture, **c** crack propagation at the PMZ

Table 1 Calculated values of elastic stress concentration factors with Eqs. 1 and 2

Parameter	Thickness t (mm)	Radius ρ (mm)	Angle θ (Lehrke)	Angle θ (Ushirokawa)	Parameter m [16]	Reinforcement width W (mm)
Lehrke	2.8	0.5	24°		0.2145	2.8
K_{t1}	1.62					
Ushirokawa	2.8	0.5		156°		2.8
K_{t2}	1.54					

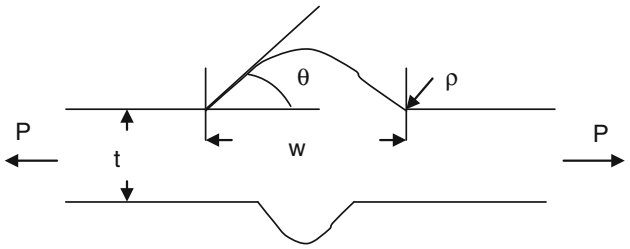

Fig. 11 Parameters in Eq. 1 for a butt weld in tension

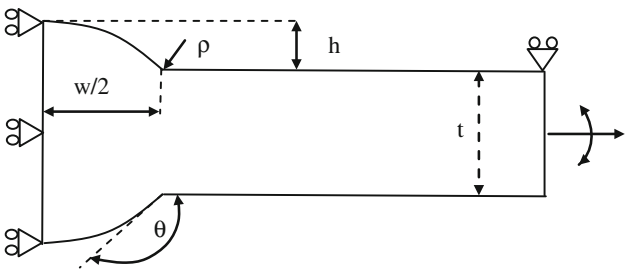

Fig. 12 Parameters in Eq. 2 for a butt weld in tension and bending

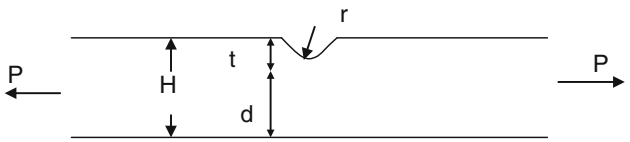

Fig. 13 Parameters used in Eq. 6 for the calculation of K_{tn}

$$Kt_n = 3.065 - 8.871(t/H) + 14.036(t/H)^2 - 7.21(t/H)^3 \quad (6)$$

The parameters t, H, d, and r used in Eq. 6 are displayed in Fig. 13. In Eq. 6 the welded joint configuration parameters $H = 2.8$ and $t = 20$ μm have been used. The notch radius of curvature has been estimated according to the maximum pit depth determined experimentally in "Results" section ($r = 11$ μm).

With Eq. 6 the resulting elastic stress concentration factor around the corrosion pit has been calculated $K_{tn} = 3.03$. The local stress, σ_{localpit}, at the bottom of the corrosion pit can be estimated with superposition of the solutions for the elastic stress intensity factors K_t and K_{tn}

$$K_{tc} = K_t K_{tn} \quad (7)$$

with

$$\sigma_{\text{localpit}} = \sigma_{\text{macro}} K_{tc} \quad (8)$$

By implementing Eq. 7 the elastic stress concentration factor results in the value $K_{\text{tc}} = 4.8$. This value is significant higher than the value calculated for the uncorroded specimens of $K_t = 1.6$.

Fatigue notch sensitivity

The fatigue notch factor due to corrosion pit can be estimated by using the fatigue strength values of $\sigma_{\text{Kuncorr}} = 100$ MPa and $\sigma_{\text{Kcorr}} = 80$ MPa for uncorroded and corroded joints, respectively. The fatigue strength values result in a fatigue notch factor due to corrosion of a value of $K_f = \sigma_{\text{Kuncor}}/\sigma_{\text{Kcorr}} = 1.25$. It shows that the effect of corrosion although important is much less severe than the one predicted with the elastic stress concentration at the corrosion pit of $K_{tc} = 4.8$. Using the values $K_f = 1.25$ and $K_{tn} = 3.03$ the fatigue notch sensitivity due to the presence of corrosion pit at the clad layer can be estimated as

$$q = \frac{K_f - 1}{K_{tn} - 1} \quad (9)$$

Using the above values the fatigue notch sensitivity results in $q = 0.125$. Considering that the full notch effect is described with the condition $q = 1$ and the no notch effect with the condition $q = 0$, the small value of 0.125 obtained, indicates that the actual notch effect introduced by the presence of the pit at the clad layer is important, but not as severe as predicted in the analysis performed in "Estimation of local stress around corrosion pit" section.

Discussion of results

The results presented in this study show that the clad layer may offer satisfactory protection of the weld metal even in

the case of unprotected weld region. The cladding works as a sacrificial anode maintaining the weld metal free of corrosion attack even after long laboratory corrosion exposure. The experimental fatigue results demonstrate that despite the clad layer protection, small corrosion pits created during corrosion exposure at the clad surface, may act as fatigue notches leading to accelerated crack initiation compared to the uncorroded samples.

The stress concentration imposed by the geometrical discontinuity at the weld toe/weld root has a predominant effect on fatigue behavior and assists fatigue crack initiation in both uncorroded and corroded welded joints. This is supported by fractographic evidence showing fatigue crack initiation at the weld reinforcement boundary for both uncorroded and corroded specimens. In the case of corroded welded joints, the local stress concentration created at the weld boundary is enhanced at the bottom of the pit due to the presence of the pit. The higher stress concentration produced at the weld boundary at the bottom of the pit in the corroded joints is responsible for a smaller crack initiation period and reduction of the fatigue life.

The local stress concentration has been calculated analytically. The results indicate a local high stress concentration of 4.8 at the bottom of the pit. This value is considerably higher than the estimated stress concentration of 1.63 due to the weld reinforcement alone. It explains the accelerated crack initiation in the corroded joints leading to shortened fatigue lives compared to the uncorroded samples. The actual fatigue life degradation in the corroded samples although important, is not as severe as predicted by the analysis, leading to a calculated fatigue notch sensitivity of 0.125.

It should be noted that in the present work the corrosion damage influence on fatigue performance is examined from the viewpoint of localized, pitting corrosion effect. Hydrogen embrittlement has also been recognized as a corrosion degradation mechanism for aluminum alloys [25, 26]. In the present paper, the authors have not considered the role of hydrogen embrittlement, since it is a diffusion-controlled process, expected to occur and influence crack growth in a local scale. Fatigue life, which is predominantly dependent on crack initiation stage, is not expected to be significantly influenced by hydrogen embrittlement, but mostly by the notch effect induced by weld reinforcement acting synergistically with small pits at the clad layer. Furthermore, it should be reminded that in the present analysis the effects of residual stresses at the weld region have not been taken into consideration due to the machining process, which is expected to cause a substantial relief. Yet, even small values of residual stresses may have an effect on the calculated fatigue lives.

Conclusions

In this work, the influence of salt fog corrosion on the fatigue behavior of cladded 6156 T4 aluminum alloy laser welded joints was investigated. The main conclusion of the work is that despite the general corrosion protection offered by the clad layer, the localized attack of the clad layer, in the form of pitting corrosion, leads to inferior fatigue performance.

In all cases, the weld reinforcement acts as a significant stress concentration site for fatigue crack initiation.

Acknowledgements This work has been supported by EU Wel-Air program under contract AST3-CT-2003-502832. The help of Mrs. Polina Taiganidou with metallography work is gratefully acknowledged.

References

1. Kermanidis AT, Zervaki AD, Haidemenopoulos GN, Pantelakis SpG (2010) Mater Des 31:42
2. Zhang Da-Q, Li J, Joo H, Lee K (2009) Corros Sci 51:1399
3. Petroyiannis PV, Pantelakis SpG, Haidemenopoulos GN (2005) Theor Appl Fract Mech 44:70
4. Velterop L (18–22 May 2003) Phosphoric sulphuric acid anodising: an alternative for chromic acid anodising in aerospace applications? NLR Report,NLR-TP-2003-210. National Aerospace Laboratory NLR, Structures Technology Department, Aluminum Surface Science and Technology, in Bonn, Germany
5. Davis JR (ed) (1993) ASM speciality handbook: aluminum and aluminum alloys. ASM International, OH, USA
6. Simulation Based Corrosion Management (SICOM) EU funded Project, FP6 Contract No. 030804, 2007–2010
7. Karlashov AV, Tokarev VP, Batov AP (1965) Fiziko-chimicheskaya Mekhanika Materialov 1(6):707
8. Genkin JM (1996) PhD thesis, Department of Materials Science and Engineering, Massachusetts Institute of Technology
9. Duquesnay DL, Underhill PR, Britt HJ (2005) Fatigue Fract Eng Mater Struct 28:381
10. Merati A (2005) Int J Fatigue 27:33
11. Bray GH et al (1997) In: Van Der Sluys WA, Piascik RS, Zawierucha R (eds) Effects of the environment on the initiation of crack growth ASTM STP 1298. American Society for Testing and Materials, PA, USA, pp 89–103
12. Chubb JP, Morad TA, Hockenhull BS, Bristow JW (1995) Int J Fatigue 17(1):49
13. Kermanidis AT, Petroyiannis PV, Pantelakis SpG (2005) Theor Appl Fract Mech 43:121
14. Wang QY, Kawagoishi N, Chen Q (2003) Scripta Mater 49:711
15. Jones K, Hoeppner DW (2006) Corros Sci 48:3109
16. ASTM E466-82 (1994) Annual book of ASTM standards, metals—test methods and analytical procedures, Section 3, vol 03.01, Metals-mechanical testing; elevated low-temperature tests; metallography. ASTM, PA, USA
17. ASTM B117-94 (1995) Annual book of ASTM standards, metals—test methods and analytical procedures, section 3, vol 03.02, wear and erosion; metal corrosion. ASTM, PA, USA
18. ASTM G1-90 (2000) Standard practice for preparing, cleaning, and evaluating corrosion test specimens. American Society for Testing and Materials, PA, USA
19. Zervaki AD, Haidemenopoulos GN (2007) Weld J 86:211

20. Masubuchi K (1980) Analysis of welded structures. Pergamon, Elmsford, NY
21. Brandt U, Lehrke H-P, Sonsino CM, Radaj D (1999) Anwendung des Kergrundkonzeptes für die schwingfeste Bemessung von Schweißverbindungen aus Aluminumknetlegierungen. Fraunhofer-Institut fuer Betriebsfestigkeit (LBF), Darmstadt (Final-Report)
22. Lehrke H-P (1999) Berechnung von formzahlen fuer Schweißverbindungen Konstruktion 51(1/2):47
23. Ushirokawa O, Nakayama E (1983) Stress concentration factor at welded joints. Ishikawaj ima-Harima Gihou (Technical Report) 23(4) (in Japanese)
24. Cole AG, Brown AFC (1958) J R Aeronaut Soc 62:597
25. Petroyiannis PV, Kermanidis AlTh, Kamoutsi E, Pantelakis SpG, Bontozoglou V, Haidemenopoulos GN (2005) Fatigue Fract Eng Mater Struct 28:565
26. Pantelakis SpG, Haidemenopoulos GN (2002) In: Proceedings of the 4th international conference on new challenges in mesomechanics, Aalborg University, Denmark